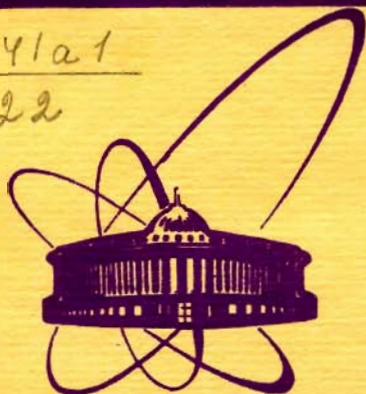


C341a1

B-22



сообщения
объединенного
института
ядерных
исследований
дубна

4888/2-79

3/12-79

E4 - 12538

J.Bang, S.N.Ershov, F.A.Gareev, G.S.Kazacha

**DISCRETE EXPANSIONS
OF CONTINUUM WAVE FUNCTIONS**

1979

E4 - 12538

J.Bang,* S.N.Ershov, F.A.Gareev, G.S.Kazacha

**DISCRETE EXPANSIONS
OF CONTINUUM WAVE FUNCTIONS**

* The Niels Bohr Institute, University of
Copenhagen DK-2100, Copenhagen Ø, Denmark.

Банг Е. и др.

E4 - 12538

Дискретные разложения волновых функций континуума.

Рассматриваются различные дискретные разложения волновых функций континуума в конечной области пространства, функций Грина, S -матрицы. Теоретически и численно исследуются свойства сходимости этих разложений в случае одночастичных состояний для потенциалов Вудса-Саксона и прямоугольной ямы. Детально обсуждаются свойства разложения по новому типу реальных функций Вайнберга. Показывается, что новый тип разложения обладает наилучшими свойствами сходимости, когда фазовый сдвиг равен фазовому сдвигу потенциального рассеяния.

Работа выполнена в Лаборатории теоретической физики ОИЯИ.

Сообщение Объединенного института ядерных исследований. Дубна 1979

Bang J. et al.

E4 - 12538

Discrete Expansions of Continuum Wave Functions

Different methods of expanding continuum wave functions in terms of discrete basis sets are discussed. The convergence properties of these expansions are investigated, both from a mathematical and a numerical point of view, for the case of potentials of Woods-Saxon and square well type.

The investigation has been performed at the Laboratory of Theoretical Physics, JINR.

Communication of the Joint Institute for Nuclear Research. Dubna 1979

Introduction

In a preceding paper, here called I, different discrete expansions of continuum wave functions in a finite region were reviewed. Their orthogonality and completeness relations were discussed and expressions for the corresponding expansions of the Green function were given.

In this paper, where we use common enumeration of equations with I, we investigate the convergence properties of the different expansions, theoretically and numerically, for the case of single particle continuum states of Woods-Saxon and square well potentials and the corresponding S-matrix. In I, a new type of real Weinberg expansions was suggested; here a more detailed discussion of its properties is given.

c. Numerical Results

The mathematical convergence properties of the pole expansions of S-matrices and continuum wave functions, shown above, are fundamental for the use of these expansions, and they also give some hints as to which expansions should be used in concrete cases. Still, some numerical comparisons between exact calculations and different expansions seem necessary in order to give a definite answer to the question of the advantages and drawbacks of the different expansions. We shall present such calculations for two cases: the square well and the Woods-Saxon potential.

The Square Well

Let the radius of the well be equal to the cut-off radius, α , the well depth V_0 .

For S-states, we now have the well-known expressions for the S-matrix and the radial wave function

$$S(k) = \frac{\alpha \cos(\alpha \alpha) + i k \sin(\alpha \alpha)}{\alpha \cos(\alpha \alpha) - i k \sin(\alpha \alpha)} e^{-2i k \alpha} \quad (3.24)$$

$$\psi_0(k, z) = \frac{k e^{-i k \alpha} \sin(\alpha z)}{\alpha \cos(\alpha \alpha) - i k \sin(\alpha \alpha)} \quad (z \leq \alpha), \quad (3.25)$$

where

$$k^2 = \frac{2m}{\hbar^2} E, \quad \alpha_0^2 = \frac{2m}{\hbar^2} V_0, \quad \alpha^2 = k^2 + \alpha_0^2.$$

It is easily seen²¹ that the resonance functions are of the form

$$\varphi_n(z) = \left(\frac{2K_n}{i + K_n \alpha} \right)^{1/2} \sin(\alpha_n z) \quad z \leq \alpha \quad (3.26)$$

$$\alpha_n \cot(\alpha_n \alpha) = i K_n \quad (3.27)$$

for ψ_0^G , we shall look at the following expressions, obtained by direct Cauchy-Mittag-Leffler expansion ($p = -1, 0, 1$)

$$\psi_{A1}(k, z)_N = -k e^{-i k \alpha} \sum_{n=1}^N \frac{\varphi_n(0) \varphi_n(z)}{2K_n (k - K_n)} \quad (3.28)$$

$$\psi_{A2}(k, z)_N = k e^{-i k \alpha} \left\{ \psi_0^G(0, z) - \sum_{n=1}^N \frac{k}{K_n} \frac{\varphi_n(0) \varphi_n(z)}{2K_n (k - K_n)} \right\} \quad (3.29)$$

$$\psi_{A3}(k, z)_N = k e^{-i k \alpha} \left\{ \psi_0^G(0, z) + [\psi_0^G(0, \alpha)]'_k \cdot k - \sum_{n=1}^N \left(\frac{k}{K_n} \right)^2 \frac{\varphi_n(0) \varphi_n(z)}{2K_n (k - K_n)} \right\} \quad (3.30)$$

and the following, obtained by the similar expansions of G in (3.22)

$$\psi_{B1}(k, z)_N = \sin(kz) + \sum_{n=1}^N \frac{\varphi_n(z) \langle K | V | n \rangle}{2K_n (k - K_n)} \quad (3.31)$$

$$\psi_{B2}(k, z)_N = \sin(kz) + \int_0^{\alpha} G^+(0, z, z') V(z') \sin(kz') dz' + \sum_{n=1}^N \frac{k}{K_n} \frac{\varphi_n(z) \langle K | V | n \rangle}{2K_n (k - K_n)}, \quad (3.32)$$

where we have

$$\psi^G(0, z) = \frac{\sin(\alpha_0 z)}{\alpha_0 \cos(\alpha_0 a)} \quad (3.33)$$

$$[\psi^G(0, z)]'_K = \frac{i}{\alpha_0^2} \frac{\sin(\alpha_0 z) \sin(\alpha_0 a)}{\cos^2(\alpha_0 a)} \quad (3.34)$$

$$\langle K | V | n \rangle = V_0 \int_0^a \sin(Kz) \left(\frac{2K_n}{z + K_n a} \right)^{1/2} \sin(\alpha_n z) dz \quad (3.35)$$

$$G^+(0, z, z') = - \frac{\sin(\alpha_0 z) \cos(\alpha_0 (z' - a))}{\alpha_0 \cos(\alpha_0 a)} \quad (3.36)$$

For large N -values, the equations (3.28)-(3.32) will often give the exact result with 3-5 correct digits. It is therefore not practical to give a direct graphical comparison between exact and approximate functions. Instead, we shall give the values of some integral expressions, which characterise the deviation of the approximate expression from the exact one. A convenient expression is, to our mind

$$\Phi_N^M(K) \equiv \int_0^a |\psi(K, z) - \psi_N(K, z)_N| dz, \quad (3.37)$$

where M can take the values $A1, A2, A3, B1, B2$, whereas N is the number of poles in our expansion ($N = \nu + n_0$, where ν is the number of bound and antibound states, and n_0 the number of poles in the fourth quadrant). Another number, which characterizes the accuracy of our expansions is the maximal error in the calculation of the wave function

$$\Delta \psi_N^M = |\psi(K, z) - \psi_N(K, z)_N|_{MAX}. \quad (3.38)$$

Note, that as a rule, this maximal error will be found at the point $z=a$.

The functions $\Phi_N^M(K)$ and $\Delta \psi_N^M(K)$ are shown in fig. 1 and 2, respectively ($V_0 = -48.72 \text{ MeV}, \beta_0 = \alpha_0 R = 5$). It is seen, that the accuracy obtained by expressions (3.28), (3.29) and (3.30) soon becomes worse, where K is enlarged, whereas the expressions (3.31) and (3.32), although they give functions, which are oscillating with K , in general are stable in a large K -interval ($0 < K < 8 \text{ fm}^{-1}$).

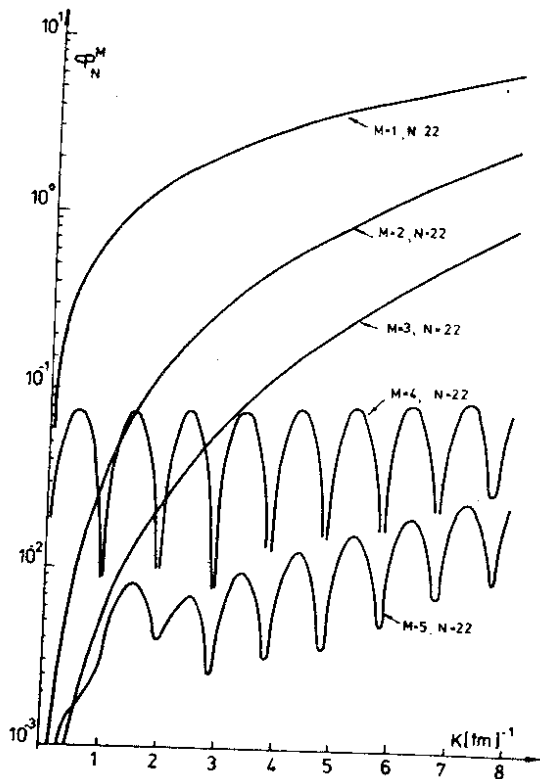


Fig. 1 The κ -dependence of the mean error $\mathcal{P}_N^M(\kappa)$ (3.37) for the different Mittag-Leffler expansions according to equations (3.28-3.32). The number of terms in the expansions is $N = 22$, the parameters given in the text. The M -values 1-5 correspond to A1, A2, A3, B1 and B2.

The best accuracy is obtained by means of the expression (3.32). For sufficiently large κ -values, the following relations are fulfilled by the errors of the difference Mittag-Leffler expansions of the continuum wave functions

$$\Phi_N^{A1} > \Phi_N^{A2} > \Phi_N^{A3} > \Phi_N^{B1} > \Phi_N^{B2}, \quad (3.39)$$

$$\Delta\psi_N^{A1} > \Delta\psi_N^{A2} > \Delta\psi_N^{A3} > \Delta\psi_N^{B1} > \Delta\psi_N^{B2}. \quad (3.40)$$

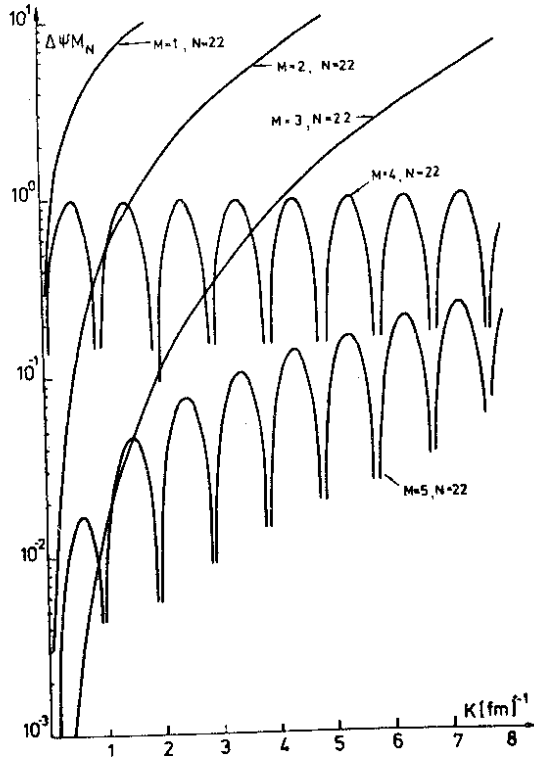


Fig. 2 The κ -dependence of the maximal error $\Delta\psi_N^M$ (3.38). Symbols and parameters as in fig. 1.

It is therefore clear, that there is in general, advantage to use the expression (3.32). In fig.3 are shown the values of Φ_N^{B2} with different numbers of poles taken into account in (3.32). The results show the rather fast convergence of this expansion.

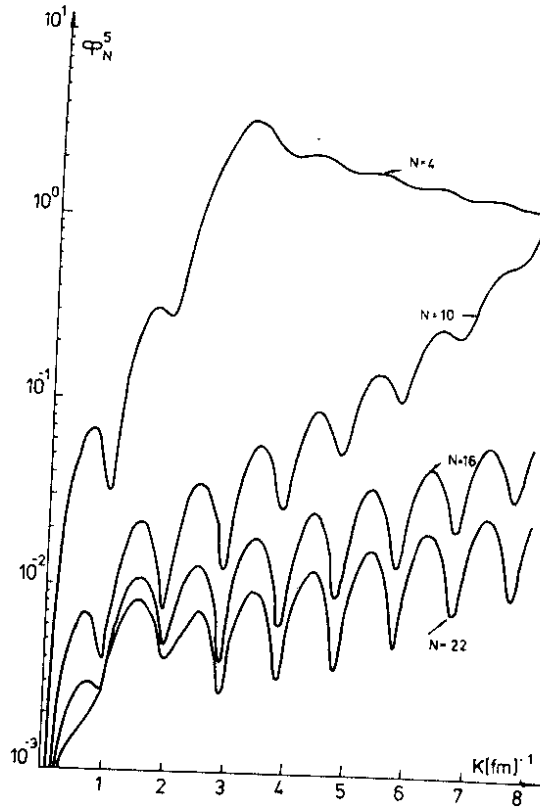


Fig. 3 The dependence on k and on the number of terms N of the mean error $\Phi_N^5(k)$ according to equations (3.32) and (3.37). Parameters as in fig. 1.

We shall further look at the different expansions (3.13), (3.15) and (3.18) for the S-matrix, which we for the concrete case shall write as

$$S^A = e^{-2i\kappa\alpha} \left[1 + \kappa S'_\alpha(0) + \frac{1}{2!} \kappa^2 S''_\alpha(0) - i \sum_{n=1}^N \left(\frac{\kappa}{\kappa_n} \right)^3 \frac{\varphi_n^2(\alpha)}{\kappa - \kappa_n} \right] \quad (3.41)$$

$$S^{B1} = 1 - 2i e^{-i\kappa\alpha} \left[V_0 \int_0^\alpha \sin(\kappa z) \Psi^G(0, z) dz - \sum_{n=1}^N \frac{\kappa}{\kappa_n} \frac{\varphi_n(\alpha) \langle \kappa | V | n \rangle}{2\kappa_n (\kappa - \kappa_n)} \right] \quad (3.42)$$

$$S^{B2} = 1 - 2i e^{-i\kappa\alpha} \left[V_0 \int_0^\alpha \sin(\kappa z) \Psi^G(0, z) dz + V_0 \kappa \int_0^\alpha \sin(\kappa z) \Psi^G(0, z)'_K dz - \sum_{n=1}^N \left(\frac{\kappa}{\kappa_n} \right)^2 \frac{\varphi_n(\alpha) \langle \kappa | V | n \rangle}{2\kappa_n (\kappa - \kappa_n)} \right] \quad (3.43)$$

$$S^{C1} = 1 - \frac{2i}{\kappa} \left[\langle \kappa | V | \kappa \rangle + \sum_{n=1}^N \frac{\langle \kappa | V | n \rangle^2}{2\kappa_n (\kappa - \kappa_n)} \right] \quad (3.44)$$

$$S^{C2} = 1 - \frac{2i}{\kappa} \left[\langle \kappa | V | \kappa \rangle + V_0^2 \int_0^\alpha dz \int_0^\alpha dz' \sin(\kappa z) G(0, z, z') \sin(\kappa z') + \sum_{n=1}^N \left(\frac{\kappa}{\kappa_n} \right) \frac{\langle \kappa | V | n \rangle^2}{2\kappa_n (\kappa - \kappa_n)} \right], \quad (3.45)$$

where

$$S'_\alpha(0) = \frac{2i}{\alpha_0} \operatorname{tg}(\alpha_0 \alpha)$$

$$S''_\alpha(0) = -\frac{4}{\alpha_0^2} \operatorname{tg}^2(\alpha_0 \alpha)$$

$$\langle \kappa | V | \kappa \rangle = V_0 \int_0^\alpha \sin^2(\kappa z) dz. \quad (3.46)$$

It is in this case convenient to introduce the relative error

$$\Delta S_M = \left| \frac{S - S^M}{S} \right|, \quad (3.47)$$

where S is the exact S-matrix (3.24), and S^M is given by one of the expressions (3.41)-(3.45). (M can take the values $A, B1,$

B2, C1 and C2). Fig.4 shows ΔS_M as a function of K for a fixed number of pole terms, $N=22$, in all expansions. It is seen, that the smallest error is obtained with the expression (3.45), and further, that the error becomes smaller when K becomes large.

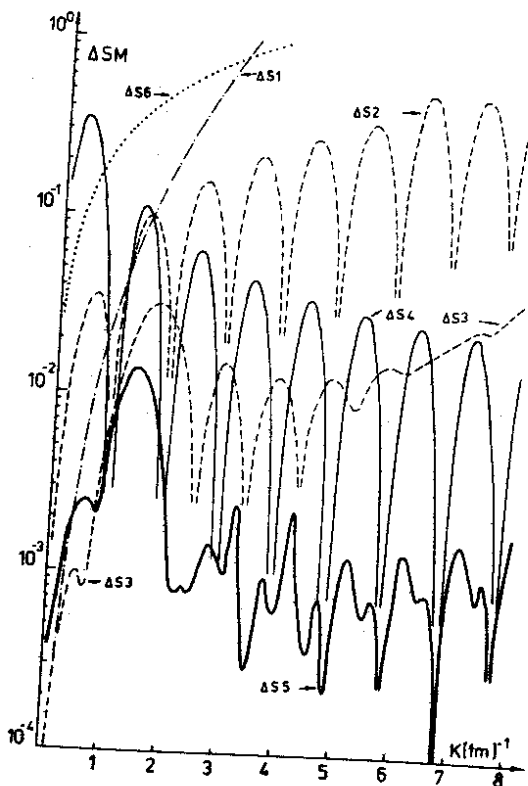


Fig. 4 The relative error of the S-matrix $\Delta S_M = \left| \frac{S - S^M}{S} \right|$, where S is the exact S-matrix, S^M is calculated by equations (3.41 - 3.45) and (3.48). Here the M-values 1-6 correspond to A, B1, B2, C1, C2, and D.

The general conclusion which can be drawn from our calculations is, that the most accurate values of the continuum wave functions and the S-matrix are obtained from those expressions, which use the Mittag-Leffler expansion of the Green function. A good agreement between the approximate results and the exact ones is in our case obtained for a very large energy interval ($0 \leq E \leq 1250 \text{ MeV}$).

It should be noted, that all the Mittag-Leffler expressions for S given above, are non-unitary, although their asymptotic behaviour for $K \rightarrow \infty$ and for $K \rightarrow 0$ is correct. It is in this connection interesting to look at the expansion of ref.³⁾ for the S-matrix, which is unitary, whereas its asymptotic behaviour, for a finite number of terms in the expansion, is incorrect. The values of ΔS^D , given by

$$\Delta S^D = \left| 1 - \frac{e^{-2iK\alpha}}{S} \prod_{n=1}^{22} \frac{K_n + K}{K_n - K} \right|, \quad \Delta S^D = \Delta S_S, \quad (3.48)$$

It is seen from fig.4 that the unitary approximation is inferior to all the others except the first one ($\Delta S^A > \Delta S^D$ for $K \gtrsim 3 \text{ fm}^{-1}$) for large energy values.

The Woods-Saxon Potential

The exponential increase of the resonance functions with z , and the increase of their number of oscillations with n , prohibits the application of the usual methods of finding eigenvalues in the case of realistic potentials. Three more refined methods of solving this problem are described in the appendix; in order to get reliable results, the three methods were combined in obtaining the numbers quoted below.

The calculations were made for a potential

$$V(z) = -V_0 f(z) + \frac{\alpha V_0}{z} \frac{df(z)}{dz}. \quad (\bar{e}, \bar{\sigma})$$

$$f(z) = \frac{1}{1 + \exp\left(\frac{z - R_0}{d}\right)}$$

with

$$R_0 = 1.24 A^{1/3} \text{ fm}, \quad A = 16, \quad d = 0.63 \text{ fm},$$

$$V_0 = 53.35 \text{ MeV}, \quad \alpha = 0.263 \text{ fm}^2.$$

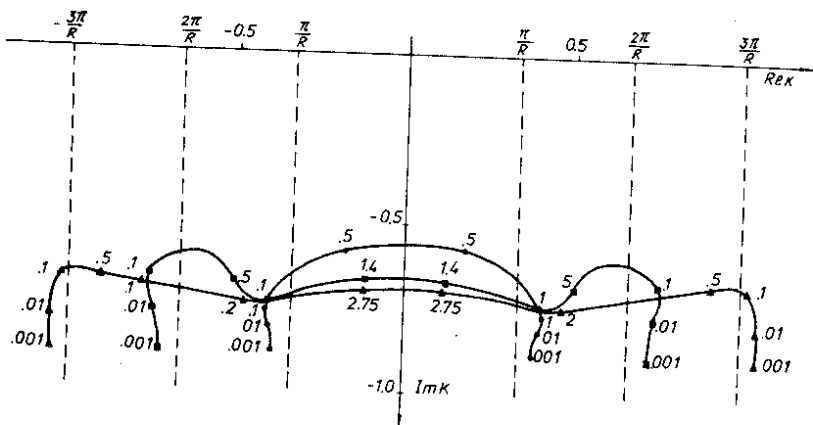


Fig. 5 The motion of the poles of the S-matrix K_n with increasing depth of the Woods Saxon potential. The numbers at the curves give the values of γ , where $\gamma V_0 = \gamma \cdot 53.35$ MeV is the depth of the potential, $\ell=0$. The black circles denote $n = \pm 1$; the squares denote $n = \pm 2$, and the triangles denote $n = \pm 3$.

It is well known^{4/}, that when we investigate the analytical properties of the solution of the Schrödinger equation, the dependence on the potential parameters of the eigenvalues is of primary importance. This dependence was earlier studied for the square well^{5/} and the screened attractive Coulomb potential only^{6/}, we are therefore in fig.5 showing the eigenvalues K_{ne} for $\ell=0$ as functions of the potential depth V_0 , keeping the order parameters constant. The cut-off radius a was $a = R_0 + 10d$. For the rectangular well, the double poles meet at $K_{n0} = -i/R$, independent of n . For the Woods-Saxon potential, the position of the double pole depends on n . The position of the single poles will in general for all ℓ -values differ from that of the poles in the square well, but with decreasing well depth we see the same characteristic picture of the motion of the poles as in the rectangular case.

For $\ell \neq 0$, the double poles are at $K_{ne} = 0$ for all potentials of the type considered, but with decreasing well depth, the motion of the poles for $\ell=1, j=3/2$ with the Woods-Saxon potential is in the same interval very different from the corresponding motion

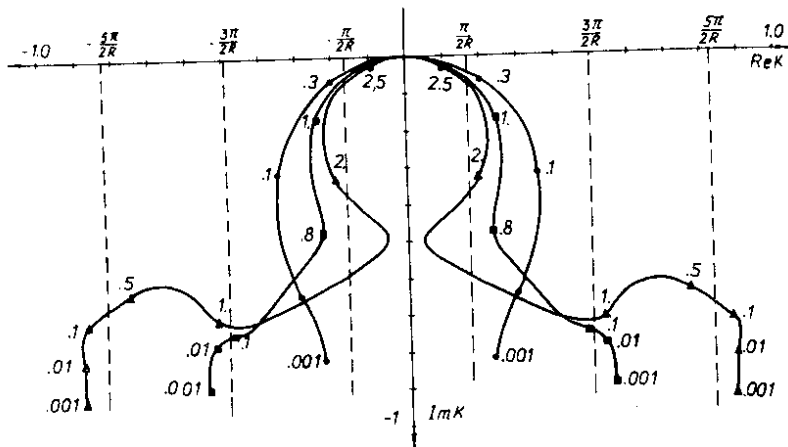


Fig. 6 The motion of the poles of the S-matrix with increasing depth of the Woods-Saxon potential for $\ell=1$, $j=3/2$ symbols as in fig. 5.

of the square well case. For very small potential values, the asymptotic behaviour of the poles is again independent of the type of the well (cfr. fig.6).

The convergence properties of the different Mittag-Leffler expansion methods was discussed above; here we shall only look at the fast converging method (3.18) in the case of $\ell=0$, with the number of poles $N=10$. In the interval $0 < K < 1.5$ ($0 < E < 45$ MeV) this expansion gives reasonably precise results (cf. fig. 7,8,9).

As a demonstration of this, the exact wave function for the case of $K=1 \text{ fm}^{-1}$ is in fig.9 shown together with the one, obtained from equation (3.23) with $N=10$. It is seen, that the real part of the approximated wave function is identical to that of the exact one, and that the deviation of the imaginary part is only 10%.

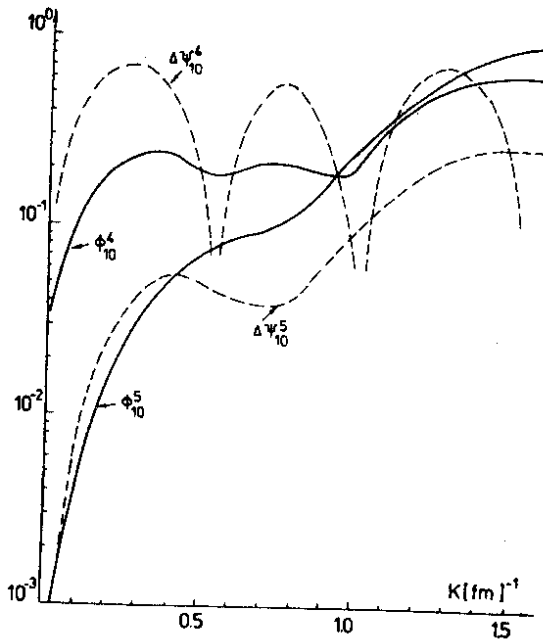


Fig. 7 The K -dependence of the mean errors $\mathcal{P}_{10}^4(k)$ and $\mathcal{P}_{10}^5(k)$, and of the maximal errors $\Delta\gamma_{10}^4(k)$ and $\Delta\gamma_{10}^5(k)$. Here, the potential is S-W with parameters given in the text, $c=0$, the number of terms in the Mittag-Leffler expansion is 10, other symbols as in fig. 1 and 2.

4. Expansions in Terms of Sturm-Liouville, Weinberg, Kapur-Feierls and Natural Boundary Conditions States

a. Formalism

The Sturm-Liouville functions, which are solutions of (2.1)-(2.6a) with γ as eigenvalue were considered in details in ref. 7/ for the case of V being a Woods-Saxon potential, and the expansion properties of these states were discussed mathematically as well as numerically.

The completeness of these states, eqs. (2.14), for the potentials in which we are interested, follows from Mercer's theorem. It was proved in ref.^{7/} that the convergence of the expansion

$$\Psi(z) = \sum_n \varphi_n(z) \langle \varphi_n | V | \Psi \rangle \quad (4.1)$$

is not only absolute and uniform, but also, for some important cases, where Ψ satisfies

$$(H_0 - E)\Psi = 0 \quad z \rightarrow \infty \quad (E < 0) \quad (4.2)$$

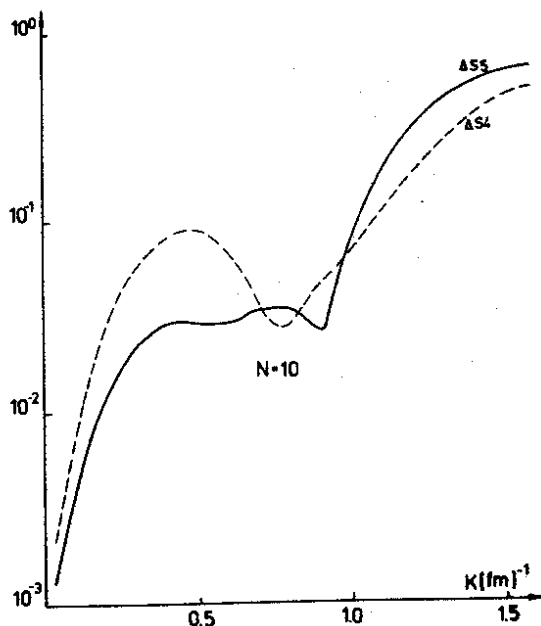


Fig. 8 The K -dependence of the relative errors of the S-matrix ΔS_4 and ΔS_5 with the same parameters as in fig. 7, symbols as in fig. 4.

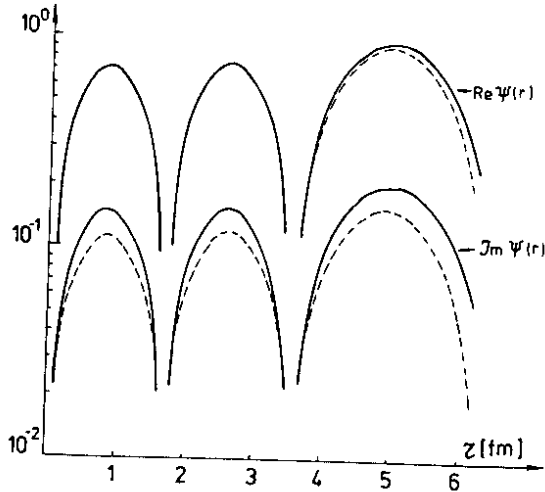


Fig. 9 The full curves represent the exact wave function for the Woods-Saxon potential of the text, $l=0$, $\kappa=1\text{fm}^{-1}$. The dotted curves are obtained with the Mittag-Leffler expansion (3.32) for $p=0$ and number of poles $N=10$.

is very fast and has the property of uniform convergence of the logarithm, i.e.,

$$\left| \frac{\psi_N - \psi}{\psi} \right| \xrightarrow{N \rightarrow \infty} 0, \quad (4.3)$$

where ψ_N corresponds to the neglect of terms with $n > N$ in (4.1).

For unbound states, an expansion in terms of Sturm-Liouville functions with $E < 0$ will not have so nice convergence properties, and we shall look for extensions of this expansion to the region of $E > 0$.

Since $G^+(E \text{ real, positive})$ is obtained from $G(E \text{ real, negative})$ by analytic continuation in E , approaching the cut from the upper plane, the expansion (2.20) is obtained from the analogue expansion of $G(E < 0)$ by analytic continuation. It is

just needed to show, that the eigenvalues, χ_i , and eigenfunctions, φ_i , of (2.1)-(2.6a) can be analytically continued along such a path. Here the only restriction is, that such E -values, which correspond to multiple poles should be avoided.

As was shown in^{2/} in the appendix, the double poles will in the square well case satisfy

$$K \frac{dh_e^+(k\alpha)}{dk} / h_e^+(k\alpha) = \begin{cases} -e \\ e+1 \end{cases}$$

It is easily seen, that this can only be fulfilled for isolated (χ, E) values, and that the same must be the case for potentials, which are similar to the square well, like the cut-off Woods-Saxon potential.

The expansion (4.1) is also analytic in E (or K), and, being an identity on the whole negative E -axis, (4.1) must also be true (and the expression absolutely convergent) for the φ_i 's, obtained by analytic continuation^{3/}. So, for our case of bounded functions in $0 \leq r \leq \alpha$, we have again completeness of the functions φ_i .

The Sturm-Liouville expansion could be generalized to positive energies in another way. Instead of conserving its analytic properties, its property of being an expansion in real functions could be conserved.

The general real-energy radial Schrödinger wave function has the asymptotic behaviour

$$\varphi_e^{\Delta_e}(k) \sim C_e \sin(kr + \Delta_e) \quad r \rightarrow \infty \quad (4.4)$$

Although we are here only considering elastic scattering in a spherical potential, (4.4) is of course true for all open channels, and we shall write the following formulae in a way, which is correct for the many-channel case.

We can obtain a solution, which contains a normalized free particle wave function, ψ_0 , added to a function, which behaves like φ^{Δ_e} for $r \rightarrow \infty$, by means of the Green function (2.24)

$$\psi^{\Delta_e} = \psi_0 + G^{\Delta_e} V \psi_0 \quad (4.5)$$

(where the Δ_e for different channels may be identical or different).

Note, that G^Δ is related to G^+ by

$$G_0^+ = G_0^\Delta + \frac{\pi e^{-i\Delta}}{\sin \Delta} \delta(E - H_0)$$

$$= G_0^\Delta + \frac{\pi e^{-i\Delta}}{\sin \Delta} \sum_{\beta} \psi_{0\beta}(E) \langle \psi_{0\beta}(E) | \quad (4.6)$$

where the sum runs over the channels in scattering.

The corresponding eigenfunctions of the Sturm-Liouville equations (2.1) - (2.6c) can be called real Weinberg functions. It can be shown^{9/} that also these functions form a complete set. Since, for the potentials we are considering here, only a finite number of the eigenvalues λ_i are negative. Mercer's theorem can again be used to show, that the corresponding expansion, given by (4.1) is absolutely and uniformly convergent.

The special case of $\Delta = \frac{\pi}{2}$, corresponding to the principal value Green function was specially investigated by Huby^{11/} and Sasakawa^{10/}. It should be noted, however, that the existence of negative eigenvalues was neglected in ref. ^{10/}, therefore the expansion (4.1) would not give the correct result.

The freedom in the choice of Δ is, however, a great advantage, if we want to expand a function, which satisfies (4.2) for $E > 0$, but for $E < 0$ satisfies an equation, different from (2.1) (say, it satisfies an equation with a residual interaction).

If ψ_e asymptotically has the behaviour

$$\psi_e \sim \sin(kr + \delta_e), \quad \frac{\hbar^2 k^2}{2m} = E, \quad (4.7)$$

the expansion will have the same convenient convergence properties, e.g., (4.3), as in the bound state case, provided the residual interactions and the potential satisfy similar conditions as in ref. ^{7/}.

Looking at the expression for the Green function

$$G^{\Delta_e} = \sum_i \frac{\lambda_i^{\Delta_e}}{1 - \lambda_i^{\Delta_e}} \psi_{e_i}^{\Delta_e} \langle \psi_{e_i}^{\Delta_e} \quad (4.8)$$

we see, that it becomes singular when $\lambda_i^{\Delta_e} \rightarrow 1$, i.e., when the homogenous equation already has a solution with the asymptotic behaviour given by (4.7) with $\Delta_e = \delta_e$

The solution of (4.5) or of the corresponding Lippman-Schwinger equation

$$\Psi^\Delta = \Psi_0 + G_0^\Delta V \Psi^\Delta \quad (4.9)$$

can be used to construct the K-, T- and S-matrices. We subtract from (4.9) the usual outgoing Lippman-Schwinger equation

$$\Psi^+ = \Psi_0 + G_0^+ V \Psi^+ \quad (4.10)$$

to obtain

$$\begin{aligned} \Psi^\Delta - \Psi^+ &\equiv D\Psi = G^\Delta V D\Psi - \frac{\pi e^{-i\Delta}}{\sin \Delta} \delta(E-H_0) V \Psi^+ \\ &= G^\Delta V D\Psi - \sum_{\beta} \frac{e^{-i\Delta\pi}}{\sin \Delta} \Psi_{0\beta} \chi_{\beta\alpha} \end{aligned} \quad (4.11)$$

from which we see, that

$$D\Psi = - \sum_{\beta} \frac{e^{-i\Delta\pi}}{\sin \Delta} \Psi_{\beta}^\Delta(E) \chi_{\beta\alpha}, \quad (4.12)$$

Here

$$\chi_{\beta\alpha} \equiv \langle \Psi_{0\beta}(E) V \Psi_{\alpha}^+(E) \rangle \quad (4.13)$$

Introducing

$$K_{\beta\alpha}^\Delta = -\pi \langle \Psi_{0\beta} V \Psi_{\alpha}^\Delta \rangle \quad (4.14)$$

we see, that we have, for the usual T-matrix

$$\pi T = -K^\Delta - \frac{e^{-i\Delta}\pi}{\sin \Delta} K^\Delta T \quad (4.15)$$

In formulae (4.6) f.f., in principle Δ operates on the channel indices, so terms like $\frac{e^{-i\Delta}}{\sin \Delta} \Psi_{\beta}^\Delta$ may be interpreted as $\frac{e^{-i\Delta_{\beta}}}{\sin \Delta_{\beta}} \Psi_{\beta}^{\Delta_{\beta}}$, etc.

From (4.15) we get

$$\pi T = -K^\Delta \left(1 + \frac{e^{-i\Delta}}{\sin \Delta} K^\Delta \right)^{-1} \quad (4.16)$$

from which we can obtain

$$S = 1 - 2\pi i T = \frac{1 + \frac{e^{+i\Delta}}{\sin \Delta} K^\Delta}{1 + \frac{e^{-i\Delta}}{\sin \Delta} K^\Delta} \quad (4.17)$$

and

$$K = \frac{\pi T}{i\pi T - 1} = \frac{K^\Delta}{1 + K^\Delta \cot \Delta} \quad (4.18)$$

Still, we may write

$$\begin{aligned} K_{\beta\alpha}^{\Delta} &= -\pi \langle \psi_{\beta} / V | \psi_{\alpha}^{\Delta} \rangle \\ K^{\Delta} &= -\pi V (1 + G^{\Delta} V). \end{aligned} \quad (4.19)$$

So, if we use the expression (4.8), we get

$$K^{\Delta} = -\pi \left(V + \sum_n \frac{\lambda_n^{\Delta}}{1 - \lambda_n^{\Delta}} V | \varphi_n^{\Delta} \rangle \langle \varphi_n^{\Delta} | V \right) \quad (4.20)$$

or using the completeness relation (2.14)

$$K^{\Delta} = -\pi \left(\sum_n \frac{V | \varphi_n^{\Delta} \rangle \langle \varphi_n^{\Delta} | V}{1 - \lambda_n^{\Delta}} \right) \quad (4.21)$$

Looking again at the elastic scattering, we see, from (4.17) with $S_e = e^{2i\delta}$ that for $\Delta \rightarrow \delta_c (+2im)$ we must have $K^{\Delta} \rightarrow \infty$, except possibly for the case of $\delta = \pi n$. This is in agreement with (2.1), (6.c), when $\gamma_n^{\Delta} \rightarrow 1$ ($\lambda_n^{\Delta} \rightarrow 1$), for $\Delta \rightarrow \delta$ or $\gamma_n^{\Delta} \rightarrow 0$ ($\lambda_n^{\Delta} \rightarrow \infty$) for $\Delta \rightarrow 0$.

From (4.6) and (4.8) we see, that also the Green function G^{Δ} is obtained as a sum of separable terms in the Δ -representation.

The expansion coefficients of $\psi_0(E)$ in the φ_i^{Δ} expansion are related to the asymptotic amplitudes, say α_i , of the φ_i^{Δ} . In fact, we have for the radial components of ψ_0

$$\left(-\frac{d^2}{dr^2} + \frac{l(l+1)}{r^2} - K^2 \right) \psi_{0e} = 0 \quad (4.22)$$

together with

$$\left(-\frac{d^2}{dr^2} + \frac{l(l+1)}{r^2} - K^2 + \frac{V}{\lambda_i} \right) \varphi_{ie}^{\Delta} = 0. \quad (4.23)$$

By multiplying (4.22) with φ_{ie} and (4.23) with ψ_{0e} , we obtain after integration and subtraction

$$\int_0^a \left(-\varphi_{ie}^{\Delta} \frac{d^2}{dr^2} \psi_{0e} + \psi_{0e} \frac{d^2}{dr^2} \varphi_{ie}^{\Delta} \right) = \frac{1}{\lambda_i} \int_0^a \psi_{0e} V \varphi_{ie}^{\Delta} dr \quad (4.24)$$

or, writing $\psi_{0e} = \sum_i c_i \varphi_{ei}^{\Delta}$

$$W(\psi_{0e}, \varphi_{ei}^{\Delta}) \Big|_a = -K \alpha_i \sin \Delta_e = \frac{c_i}{\lambda_i}. \quad (4.25)$$

Expansions in terms of Kapur-Peierls and natural boundary condition states were investigated by many authors, more

numerically as well as mathematically. These studies also include potentials of the type we are looking at, and residual interaction of different types.

Here, where we are only considering the simple (but rather fundamental) problem of the convergence of the different expansions in the case of elastic scattering, we shall concern ourselves with the Kapur-Peierls and NBC functions only for the square well ($V(z) = -V_0, z \leq z_0, V = 0, z > z_0$). Here, these states are equivalent to the corresponding Weinberg states, when the basic radius, α , is identical to the radius of the potential, z_0 . Actually, we have, with boundary condition (2.6a) or (2.6c), that the λ_i of the Weinberg case is related to the K_i of the Kapur-Peierls case by

$$\frac{V_0}{\lambda_i} \Big|_W - V_0 = K_i^2 \Big|_{K-P(NBC)} - K^2. \quad (4.26)$$

So the wave functions of the two cases are also identical, up to a common normalization factor

$$\varphi_i^W = \sqrt{V_0} \varphi_i^{K-P(NBC)} \quad (4.27)$$

Conclusion

The convergence of the different discrete expansions of continuum wave functions was investigated here for the case of potential scattering only. The usefulness of these expansions is generally connected with more complicated problems where the Hamiltonian contains residual interactions. In such cases, similar convergence properties must exist, as can be argued from the convergence of the Green functions.

The convergence of the real Weinberg expansion will be investigated in a forthcoming, in connection with some realistic potentials. The new variant of this expansion, which was introduced here, is shown to be extremely fast convergent, when Δ approaches δ . Also for more complicated scattering problems, with residual interactions, both numerical and mathematical facts speak in favour of this expansion as being fastest converging in the largest range of ξ -values.

In some problems, the fact that this basis set is energy dependent may be a drawback. In such cases, the Mittag-Leffler expansions could be advantageous, particularly when the extra term is used to speed up convergence.

References

1. J. Bang, S.N.Ershov, F.A.Gareev, G.S.Kazacha. Communication JINR, E4-12497 (1979).
2. J. Bang, F.A.Gareev, M.H.Gizzatkulov and S.A.Goncharov. Nucl. Phys. A309 (1978) 381;
J. Bang and F.A.Gareev. Communication JINR, E4-11902 (1978);
J. Bang, S.N.Ershov, F.A.Gareev. Preprint NBI-79-5 (1979).
3. Ning Hu. Phys. Rev. 74 (1948) 131.
4. R.G.Newton. Scattering Theory (Mc Graw-Hill, New York 1966)
5. H.M.Nussenzweig. Nucl. Phys. 2 (1954) 499.
6. E.M.Ferreira and A.F.F.Teixeira. J. Math. Phys. 7(1966)1201.
7. J. Bang and F.A.Gareev. Phys. Scripta 18(1978) 289, 297.
8. K.Meetz. J. Math. Phys. 3(1962)690.
S.Weinberg. Phys. Rev. 131(1963)440.
9. T.Kato. Prog. Theor. Phys. 6 (1951) 394.
10. T.Sasakawa. Supplement of Prog. Theor. Phys. 61(1977)135;
Nucl. Phys. A160 (1971)321.
11. R.Huby. Nucl. Phys. A138(1969)442; Q.Liu,
Z. Phys. 258(1973)301.

Received by Publishing Department
on June 12 1979